FRONT MATTER

Generic High-Capacity Electrochemical Capture and Release of Proteins by Polyelectrolyte Brushes

Authors

G. Ferrand-Drake del Castillo, Z. Adali-Kaya, R. L. N. Hailes, K. Xiong and A. Dahlin*

Affiliations

Department of Chemistry and Chemical Engineering
Chalmers University of Technology
41296 Gothenburg, Sweden
E-mail: adahlin@chalmers.se

Abstract

Capture and release of proteins by an electrical signal is of general interest but methods have proven difficult to develop. We present a polyelectrolyte brush electrode with high-capacity (several $\mu g/cm^2$) for protein immobilization that captures and releases proteins by an electrochemical potential. The electrochemical potential produces an interfacial pH gradient that enables rapid and tunable switch of the interaction between the polyelectrolyte brush and proteins on-demand. Key to our solution is an electrochemically inert aryl anchor between the polyelectrolytes and the electrode, which enables multiple capture-release cycles (without any regeneration step) and minimal degradation of the electrode. For all proteins tested we observed complete release by electrochemistry. In addition to proteins, the electrode could successfully immobilize and release liposomes suggesting additional applicability within the field of biomedicine and drug delivery. Importantly the electrode retained its functions when exposed to serum suggesting it can be used in a biological environment. We predict that this technology will be highly useful for protein purification and in biomedical devices.

MAIN TEXT

Introduction

Surfaces functionalized with stimuli-responsive polymers are important in a variety of applications, especially with the ability to quickly switch chemical property on demand.[1] One highly desired feature is controlled capture and release of proteins.[2-3] This is of broad interest as it relates to applications in purification,[2, 4-5] bioanalytics,[6-7] enzymatic catalysis,[8-9] lab-on-a-chip,[10] and importantly in new drug-delivery technologies[1, 11]. Proteins (in particular antibodies) now constitute most new therapeutic drugs,[12-13] which calls for new methods to achieve efficient immobilization and controlled release in biological environments.[4-5, 12-13] A useful protein capture-and-release technique should ideally combine: high immobilization capacity, on-demand tunable release, re-usability, retained function in biological fluids, and preserve the structure and function of the proteins. However, incorporating even some of these features into one technical solution has proven challenging.

A promising strategy to trigger protein interactions with surfaces is by use of electrochemical signals.[11, 14-15] Electrochemical activation is appealing since it provides a simple way of tuning the dose,[16] it is compatible with miniaturized devices,[17] it can be performed remotely,[18] and if the electrode does not degrade from electrical signals it could be re-used[14]. Several interfaces have been developed for the immobilization and release electrochemically on-demand of small molecules,[19-21] DNA,[22-23] insulin,[24] or even whole cells[25] by using a variety of chemical interactions. In a particularly relevant case His-tagged proteins were released from graphene electrodes by electrochemical signals.[15] But, catch and release designs often use interfaces that are not compatible with proteins, which require gentle immobilization methods to preserve their structure and biological activity.[26-27] One exception to this is the use of specific receptors designed to capture a particular protein; these can sometimes be combined with changes in the chemical environment to provide release.[28] Unfortunately, such affinity-based methods have extreme requirements for the receptor:[29] they must keep the target proteins securely bound and immobilized at high density, whilst preserving activity etc. Many of the electrodes designed for release are planar two-dimensional monolayer surfaces with inherently low protein binding capacity.[6, 15, 21, 25] Although polymer hydrogels and brushes with high binding capacities exist, successful examples anchored to electrodes have yet to be demonstrated for electronically controlled protein catch and release.[6, 30-32] One way to improve the capacity for release is to store molecules in microcontainers sealed by thin membranes than can be dissolved electrochemically.[17-18] Although this approach is promising for many compounds, it has rarely been used for proteins and requires advanced microfabrication. Furthermore, most existing release techniques are limited to single use since the whole chemical construct is removed.[20, 22, 25]

Here we present our new concept for electrochemical capture and release of proteins from polyelectrolyte brushes (Fig. 1). Central to our concept is the use of polyelectrolyte brushes that switch reversibly by electrochemistry. Our solution fulfills all the above stated desired features of a protein capture and release system.

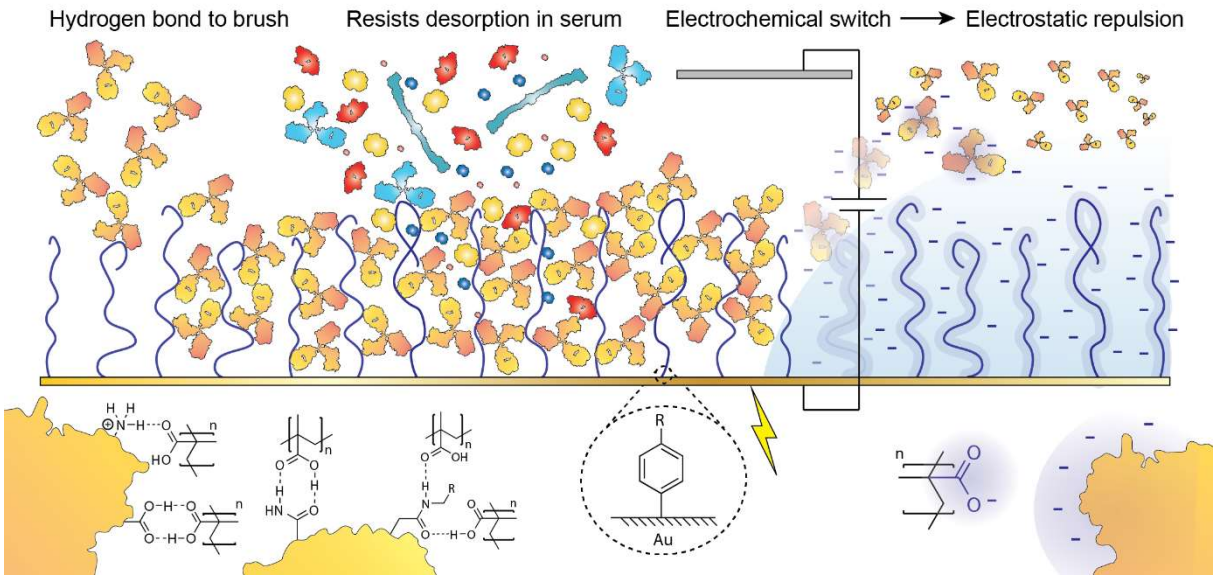

Fig. 1. Generic concept for capture and electrochemical release of proteins exemplified with antibodies. Proteins hydrogen bond to neutral, weak polyacidic brushes. The loaded brush resists spontaneous protein desorption when exposed to serum. Upon applying an electrochemical signal an interfacial pH gradient is produced, charging the polyelectrolyte brush and inducing protein release. The electrochemically inert aryl anchor prevents de-grafting of the brush upon application of electrochemical potentials.

Results

We prepared poly(methacrylic acid) (PMAA) brushes on gold surfaces by surface-initiated activator-regenerated atom transfer radical polymerization (ATRP). Prior to polymerization, a diazonium salt[33] was synthesized (Fig. S1) and reduced by ascorbic acid to generate a covalent link to gold. The film was converted to an ATRP initiator layer, after which ATRP was performed (Fig. 2A). The weak polyacidic brushes had dry thicknesses in the range of tens of nm as determined by surface plasmon resonance (SPR).[34] We found that our surface functionalization protocol provided a polymer anchor which was stable during electrochemical potential sweeps, while still allowing Faradaic reactions. Electrochemical quartz crystal microbalance (QCM) data showed that the brushes could be fully switched between neutral and charged state by potential control, i.e. the response was the same as when performing liquid exchange with buffers that had pH well above and below the brush pK_a (Fig. 2B and C). Remarkably, the switching was very fast (<1 s) even in a buffered environment, fully reversible, and without any indication of polymer desorption.

To switch brushes from charged to neutral a positive potential was applied in the presence of a redox active species to generate protons (Fig. 2B).[35] A local reduction of pH was produced with multiple different redox species including dopamine, but hydroquinone most readily reacted to produce a rapid acidification (Fig. S2). Switching brushes to the charged state was possible by applying reductive potentials that increase the local pH by consumption of protons and oxygen (Fig. 2C):[14]

$$O_2 + 4H^+ + 4e^- \rightarrow 2H_2O$$

$$O_2 + 2H^+ + 2e^- \rightarrow H_2O_2, \qquad H_2O_2 + 2H^+ + 2e^- \rightarrow 2H_2O$$

The formation of an aryl diazonium monolayer, produced by reduction with ascorbic acid, makes the electrode surface highly accessible and enables electrochemical reactions. Electrografting, which is the established procedure, produced multilayers of aryl diazonium and blocked electron transfer (Fig. S3).[36] Thiol-based anchoring resulted in rapid polymer desorption at negative potentials as observed by in-situ electrochemistry experiments with SPR and QCM[20] (Fig. S4). The brushes were significantly harder to switch in buffers purged with nitrogen (Fig. S5), which confirms that the effect originates from the omnipresent O_2 in aqueous solutions (~0.3 mM at NTP).[14] We observed no influence from the liquid flow rate in the cell on the switching capability.

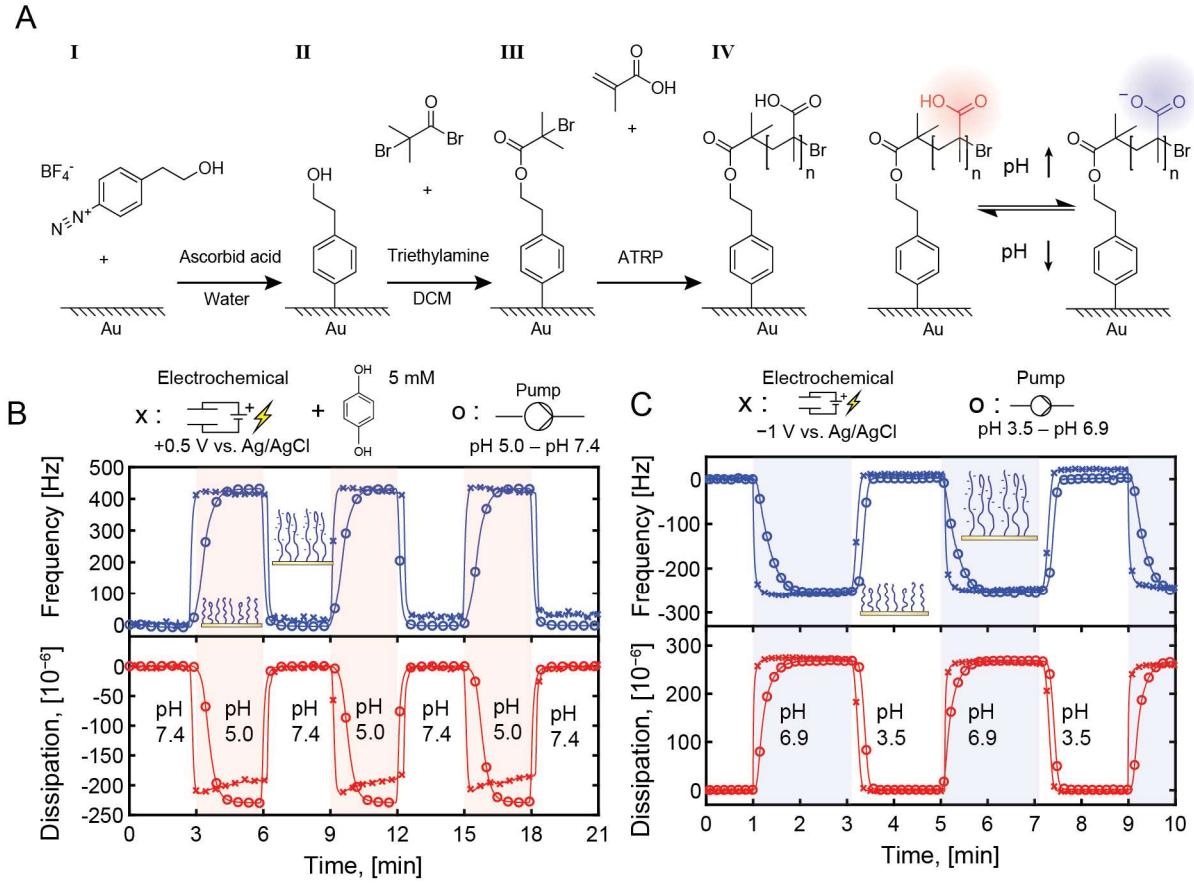

Fig. 2. Brush synthesis and characterization of local pH switching in both directions by electrochemistry. (A) Synthesis of the electrochemically stable and pH-responsive brush interface. **(B)** Electrochemical brush switching from high to low pH monitored in QCM showing brush collapse induced by applying +0.5 V in PBS and 5 mM hydroquinone. **(C)** Electrochemical brush switching from low to high pH (opposite of **B**) monitored in QCM showing brush collapse induced by applying −1.0 V in PBS. The response from changing the buffer pH by pumping is shown for comparison.

We have previously reported how proteins immobilize in high quantities to neutral PMAA at pH 5.0 and completely desorb from the brush if the pH is increased.[37] This in conjunction with the fact that we can electrochemically switch the brush (Fig. 2 B and C) suggest that controlled capture and release of proteins is possible by inducing local pH changes via electrochemical signals. Capture of BSA from solution occurs when we apply a constant electrochemical signal to lower the pH followed by instant release of bound BSA when the signal is turned off (Fig. 3 A), clearly confirmed by comparing to a control solution

containing no BSA. Capture and release of IGG (Fig. 3 B) is achieved by doing the opposite: spontaneous immobilization followed by electrochemical release, this time performed by sweep voltammetry. These show how this release technique can be both tunable and on-demand. Multiple capture and release cycles are possible since desorption regenerates the brush, shown by the QCM signal returning to baseline. As expected, the voltage required for protein release depended on the buffering capacity of the solution (Fig. S6). For proteins with high pI (e.g. avidin), the negative potential had to be applied for a longer time to raise the pH sufficiently, but all proteins tested could be fully released (Fig. S7).

In addition to proteins and PEG-modified compounds (reported previously),[37] we also bound multilayers of liposomes (Fig. 3C) without the need for tethers.[38] The ability to bind PEG and liposomes expands the use of this technique to molecules that do not spontaneously hydrogen bond to PMAA, either by conjugation to PEG or by insertion into liposomes. It also suggests high potential for applications in drug delivery where PEG-modified compounds and liposomal carriers are common.

High demands are placed on electrodes to remain functional in biological environments.[7, 39-41] Biofluids are highly crowded and rapidly interact with the electrode surface (total serum protein concentration ~70−90 mg/mL)[42]. Binding a high quantity of protein could block the electrode and hinder mass transport of oxygen and protons to the electrode surface. This would inhibit electrochemical reactions and inactivate the mechanism for release. However, our electrode remains functional even under crowded conditions (Fig. 3 A-D) and the ability to drive the electrochemical reaction i.e. mass transport of reactants to the electrode surface, is not lost. When loading electrodes with serum proteins (Fig. 3 D) the molecular crowding inside the brush at the electrode interface is comparable to the injected serum concentration (~50 g/L). Yet, the electrode is clearly capable of releasing protein (Fig. 3D) immediately by application of an electric signal indicating: (i) mass transport is not hindered; (ii) biofluid exposure does not limit electrochemical switching of the polyelectrolyte brush. Additionally, despite exposure to serum, full protein desorption occurs upon electrochemical switching. The brush returns to its original state prior to protein loading, and can then be re-used.

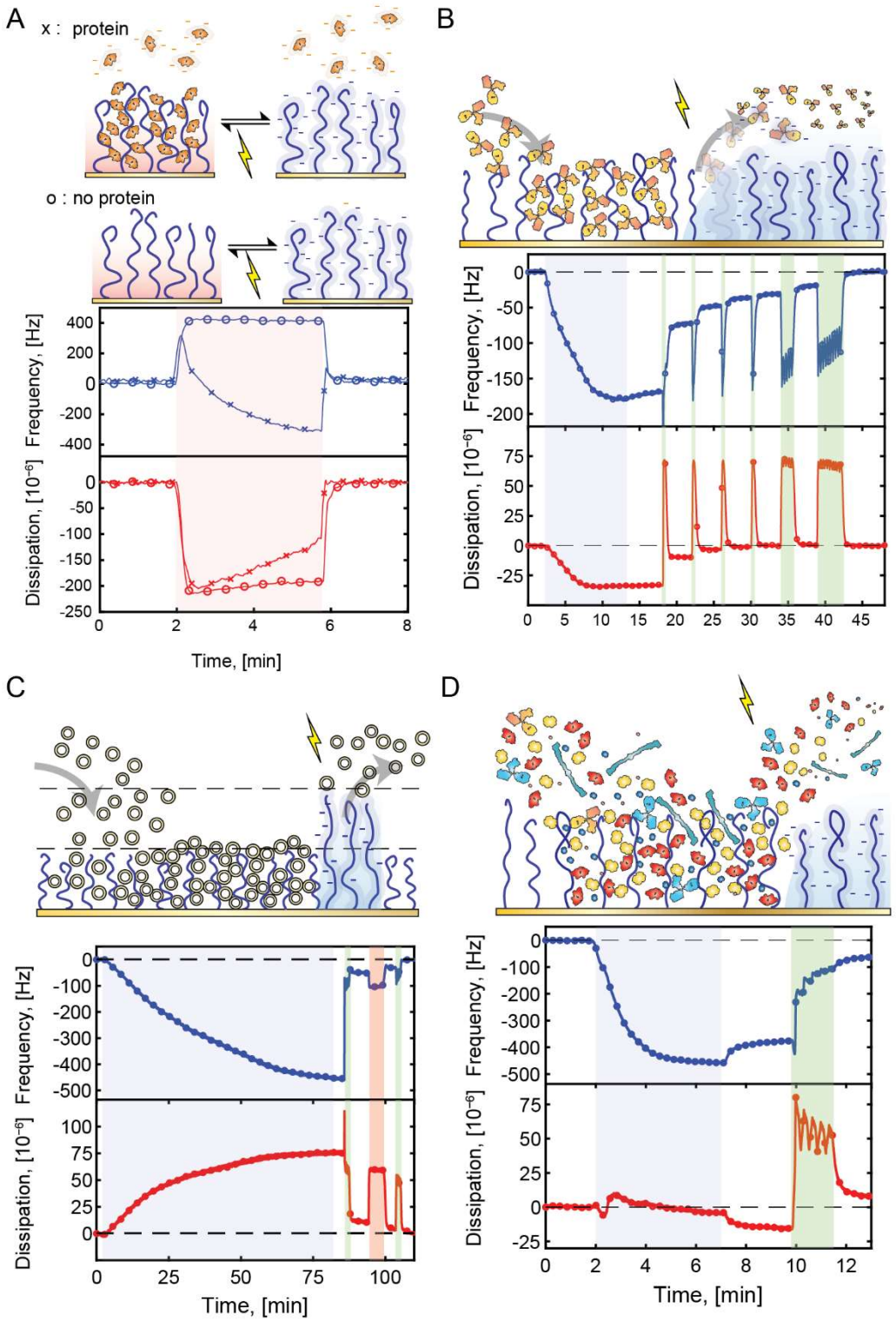

Fig 3. Electrochemical catch-and-release of proteins monitored with QCM. (A) Protein adsorption on demand occurs when applying an electrochemical potential in the presence of BSA, compared to buffer without proteins. **(B)** Tunable stepwise release of IgG in real-time. **(C)** Electrochemical release of multilayers of liposomes. **(D)** Capture of serum proteins followed by subsequent electrochemical release.

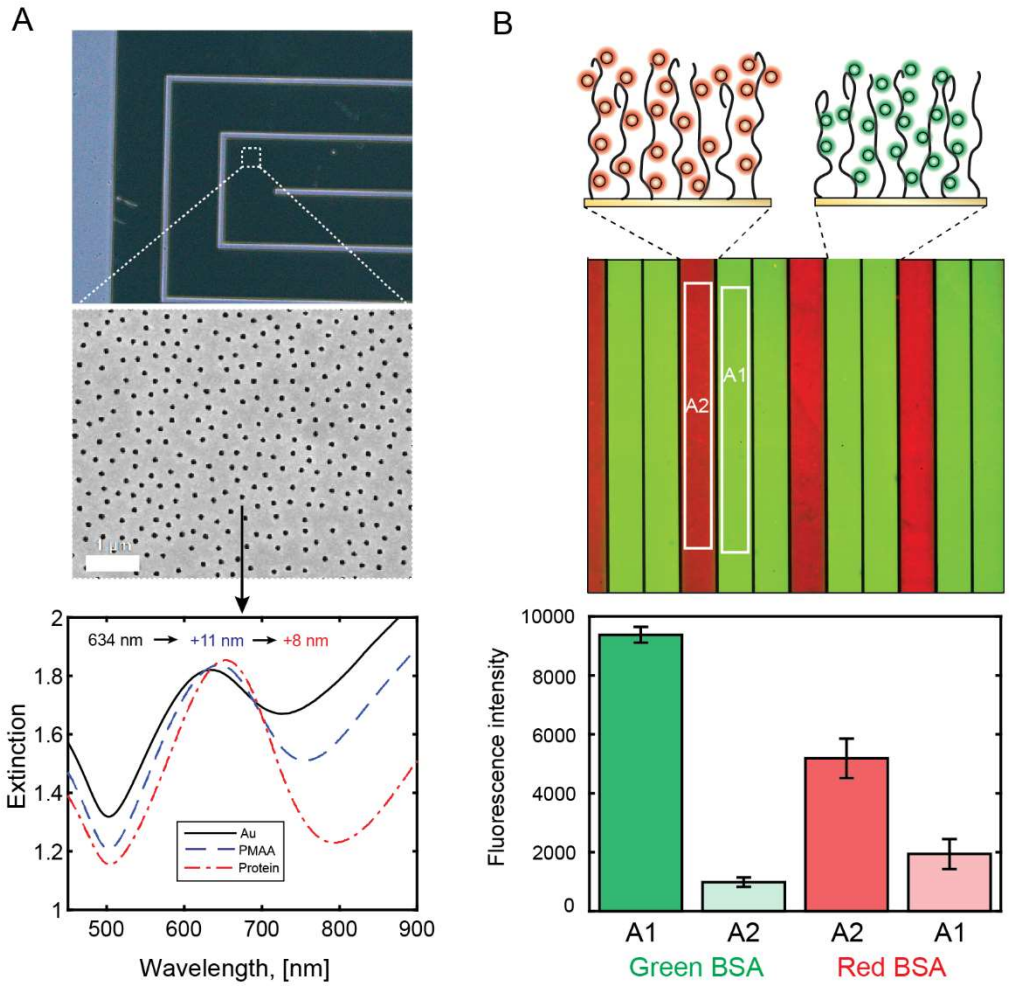

Fig 4. Protein capture and microelectrode nanostructured electrode. (A) Photo of microelectrodes (100 µm wide) and electron micrograph of nanoholes (scale bar 1 µm). The resonance peak shift in the extinction spectrum confirms brush synthesis and protein immobilization on the nanostructured gold. **(B)** Fluorescence from microelectrode stripes after local release and patterning by a second immobilization step.

To demonstrate localized release we used microelectrodes with plasmonic nanohole arrays. We confirmed protein capture in brushes by extinction spectroscopy (Fig. 4C).[43] It was possible to release a selected protein on demand from one electrode, then selectively immobilize a different protein type on the same region (Fig. 4D). These immobilization steps enable the generation of protein patterns. Several strategies for protein patterns and arrays have already been developed[6, 44-47] but many techniques are based on forming monolayers, which limit the immobilization capacity and decrease the protein activity compared to proteins bound to brushes.[48] If covalent conjugation or strong biological interactions are utilized for patterning, modifying or rearranging biomolecules on the surface carries the risk of degrading the biomolecule or the surface. The immobilization technique employed here, with high surface coverage and high retention of structure and activity, enables a dynamic and functional surface.[37] We predict our tool for local control of protein concentrations could become useful in applications requiring dynamic changes in surface chemistry. One example would be tailored enzyme cascade reactions on surfaces where protein gradients used to tune the cascade reaction and pH gradients to regulate activity are both desirable.

In this work gold surfaces were modified, but the method is applicable to a great variety of materials.[36] Similarly, whilst we have only used planar surfaces or nanohole arrays, storage capacity can naturally be increased even further by employing microstructured or porous surfaces with higher effective area. Mesoporous materials are especially interesting scaffolds since like these can be readily functionalized with brushes to enable high capacity immobilization of proteins.[32]

Conclusion

In summary, we have presented a new method for electronic catch and release of proteins and liposomes via electrochemical control of interfacial polymer brush pH. Switching can be performed over many cycles with no loss in performance. The key to successful electrochemical control lies in the diazonium-based chemical anchor used to graft the polymers to the surface. Our electrode enables high-fidelity control of protein species in space and time. We predict several application areas for this technology; implementation should be straightforward in separation technologies and analytical devices where proteins are central. Since proteins remain bound in physiological fluids and are released on demand by reduction of native oxygen, we envision utilizing the technology for controlled release of therapeutic proteins from electrodes in implanted devices.

Materials and Methods

Chemicals:

All chemicals and proteins used were purchased from Sigma-Aldrich unless stated otherwise. Water was ASTM research grade Type 1 ultrafiltered water (milli-Q-water). H_2O_2 (30%) and NH_4OH (28–30%) were from ACROS, while H_2SO_4 (98%) and ethanol (99.5%) were from SOLVECO. Chemicals used for synthesis were 4-aminophenethyl alcohol, tetrafluoroboric acid (48% solution in water), acetonitrile, tert-butyl nitrate, and diethyl ether L-ascorbic acid, dichloromethane, triethylamine, α-bromoisobutyryl bromide, tert-butyl methacrylate, dimethylsulfoxide, dichloromethane, methane sulfonic acid, *N*,*N*,*N*′,*N*″-pentamethyldiethylenetriamine (PMDTA), $CuBr_2$. Buffers used in this work were based on phosphate buffered saline (PBS) tablets (0.01 M phosphate, 0.13 M NaCl, pH 7.4) or disodium hydrogen phosphate and NaCl titrated to a specific pH with HCl (1 M aqueous solution) or NaOH (1 M aqueous solution). The lipids phosphatidylcholine and dipalmitoylphosphatidylcholine, used to prepare liposomes, were obtained from Avanti Polar Lipids.

The proteins used in this study were avidin (AVI, ThermoFisher), bovine serum albumin (BSA), BSA-fluorescein isothiocyanate conjugate, fibrinogen (FIB) from bovine plasma, glucose oxidase (GOX) Type VII G2133 from Aspergillus Niger, glucosidase (GLU), horse radish peroxidase (HRP, ThermoFisher), insulin (INS), INS glargine (INS-GLA), IgG antibodies from human serum, myoglobin (MYO) from horse skeletal muscle, lysozyme (LYS), NeutrAvidin (NAVI, Pierce), and ubiquitin (UBI) from bovine erythrocytes. Human serum (from human male AB plasma) was filtered through a 40 μm hydrophilic filter and diluted ten times in PBS prior to use. Alexa Fluor™ 488 and 555 labeling kits (ThermoFisher) were used produce different color BSA to demonstrate protein pattering.

The redox active species tested were hydroquinone, dopamine hydrochloride (DOPA), ascorbic acid, 4-aminophenethyl alcohol (tyrosol), 3,4-dihydroxyphenetylacetic acid (DOPAC), and β-nicotinamide adenine dinucleotide, reduced disodium salt hydrate (NADH).

Diazonium salt synthesis:

The synthesis of diazonium salt (Fig. S1) involved a modified literature procedure.[33] Under an inert atmosphere, 4-aminophenethyl alcohol (2.94 g, 20 mmol) and tetrafluoroboric acid (48% solution in water, 9.94 g, 113 mmol) were dissolved in acetonitrile (20 mL). In a separate flask, tert-butyl nitrate (2.269 g, 22 mmol) was dissolved in acetonitrile (12 mL). Both solutions were degassed and cooled to −20 ºC alongside 200 mL of diethyl ether. After 20 min the solutions were warmed to 0 ºC, before the tert-butyl nitrate solution was added to the 4-aminophenethyl alcohol solution dropwise with stirring. The reaction was then stirred for a further 1 h. The reaction was terminated by dropwise addition of the dark yellow solution to rapidly stirring diethyl ether (200 mL). After additional stirring for 1 h the supernatant was decanted off. The brown colored precipitate was dried and 3.69 g of impure diazonium salt was obtained and carried forward without further purification. To verify the product, 1H NMR spectra were recorded at ambient temperature on a Varian 400 MHz NMR spectrometer. Spectra were analyzed relative to external TMS and were referenced to the most downfield residual solvent resonance (CDCl3: δH 7.26 ppm). ^{1}H NMR resonances of the diazonium salt matched those previously reported[33] and analysis revealed a purity of 80%.

Surface cleaning:

Prior to surface functionalization, QCM sensor crystals (standard Au, purchased from Biolin Scientific) and SPR sensor surfaces (standard Au, purchased from BioNavis) were cleaned with piranha wash (H_2SO_4:H_2O_2, 3:1 v/v) for 10 min followed by rinsing in milli-Q. Next, an RCA1 wash (H_2O:H_2O_2:NH_4OH 5:1:1 v/v at 75 °C) was performed for 20 min, followed by further rinsing in milli-Q, sonication in ethanol, and drying with N_2. For microelectrodes the piranha wash step was omitted to prevent destruction of the surface due to delamination of the gold film with nanoholes.

Surface activation:

Gold surfaces (QCM and SPR sensors) were placed in a glass jar with a septum seal containing diazonium salt 1 (0.301 g, 1.28 mmol) and the jar was purged with N_2. In a separate flask, ascorbic acid (0.028 g, 0.16 mmol) was dissolved in water (40 mL) and the solution was degassed for 1 h. Then, the ascorbic acid solution was transferred into the sealed glass jar causing dissolution of the diazonium salt. The gold surfaces were stirred in the solution for 1 h by use of a platform shaker (nitrogen bubbles that appear on the surface after 15 min indicate successful diazonium salt monolayer formation), after which they were thoroughly rinsed in water then ethanol, and dried. To convert the diazonium monolayer into a polymerization initiator layer, the gold surfaces were exposed to α-bromoisobutyryl bromide (0.222 mL, 1.80 mmol) and triethylamine (0.302 mL, 2.17 mmol) in dichloromethane (20 mL) for 10 minutes, after which surfaces were rinsed in ethanol and dried under N_2.

Surface-initiated polymerization:

ATRP was used to prepare PMAA polymer brushes in a manner similar to published procedures.[34] Inhibitor was removed from the monomer tert-butyl methacrylate using an alumina column, after which it were stored at −20 °C, then warmed to room temperature immediately before use. Reactions were carried out using standard Schlenk line techniques under an inert atmosphere of N_2. $CuBr_2$ (0.006 g, 0.03 mmol), and PMDTA (0.052 mL, 0.246 mmol) were dissolved in dimethyl sulfoxide (20 mL) and, alongside a separate flask of tert-butyl methacrylate (20 mL, 0.1231 mol), was deoxygenated via vigorous bubbling of N_2 for 30 min. The reaction solution and monomer were then transferred via cannula into a screw-top jar (with rubber septa lid) containing initiator-prepared gold surfaces. The reaction was initiated by the addition of ascorbic acid (0.033 g, 0.185 mmol). The final concentrations of each component in the reaction medium were: [monomer] = 3.1 M, [CuBr2] = 0.6 mM, [PMDTA] = 6.2 mM, and [ascorbic acid] = 4.6 mM. The reaction was placed under magnetic stirring. Reactions were quenched by immersing the samples in pure ethanol. Poly(tert-butyl methacrylate) (PTBMA) brushes were then converted to PMAA by exposure to 0.2 mM methane sulfonic acid in dichloromethane (10 mL) for 15 min, followed by rinsing in dichloromethane and ethanol. For PAA, tert-butyl acrylate was used as the starting monomer with an otherwise identical protocol.

Quartz crystal microbalance:

Sensor crystals coated with gold were used and measurements were performed using a Q-Sense E4 (Biolin Scientific). All data shown corresponds to the first or third overtone. A flow cell with an electrochemical module (QEM 401) was used to perform in-situ electrochemical experiments. A Gamry Interface 1000E potentiostat (Gamry Instruments) was connected to

the electrochemical cell. For every experiment the internal resistance of the circuit was measured (Get Ru) and the open circuit potential was measured to verify an acceptable reference electrode performance and correctly connected circuit. The reference electrode used was a World Precision Instrument low leakage "Dri-ref" electrode. The scan rate in CV experiments was, unless stated otherwise, 100 mV/s.

Surface plasmon resonance:

Measurements were performed on a SPR Navi 220A instrument (BioNavis), both in air and in water. The total internal reflection (TIR) and SPR angle was recorded on three different laser wavelengths and in two different flow channels. The flow rate of buffer used was 20 μL/min. Electrochemical SPR measurements were performed by connecting a potentiostat (same as for QCM) to a cell designed for this purpose (from the instrument manufacturer). The methodology of analyzing SPR spectra by Fresnel modelling and the quantification has been described in previous work.[34] In brief, the refractive index of the dry polymer brushes was assumed to be equal for PAA and PMAA and set to 1.522. The deposited diazonium layer was assumed to have refractive index 1.5 (typical for organic coatings). The refractive index of dry proteins bound in polyelectrolyte brushes was assumed to be equal to that of the polymer. To obtain surface coverage, the densities of the dry polymers and proteins were set to 1.22 g/cm^3 and 1.35 g/cm^3, respectively.

Plasmonic detection with nanohole arrays:

Extinction spectroscopy was performed to detect the resonance shift of the peak.[43] In brief, the surface was imaged by a tungsten lamp in transmission mode and a fraction of the light was directed to the opening of an optical fiber in the focal plane. The detection spot (typically 50 μm) depends on the fiber diameter and the objective magnification. A fiber coupled photodiode array spectrometer (B&WTek) analyzed the spectrum. The final resolution is almost as high as in SPR (down to 0.1 ng/cm^2). Note that all data presented as resonance shifts in nm are from plasmonic nanohole arrays, while resonance shifts in degrees are from conventional angular SPR.

Fabrication of microelectrodes:

To create microscale stripe electrodes, a laser writer (Heidelberg Instruments DWL 2000) was used. The photoresist (LOR3A) was spin coated at 4000 rpm and baked on a hotplate at 180 °C for 5 min. A second layer of S1813 was spin coated at 4000 rpm and baked on a hotplate at 120 °C for 2 min. The pattern was written by a 60 mW laser beam after which the sample was developed in developer MF-318 for 50 s. The nanohole array was then prepared by colloidal lithography.[43] Finally, lift-off was performed in remover RM-Rem400.

Ex-situ electrochemical desorption of proteins

For simplicity, in some experiments protein immobilization and release was not monitored in real-time. Instead, the surfaces were immersed in a solution of proteins for 30 min to ensure saturated binding, using the kinetics from SPR and QCM measurements as guideline. Following protein loading the surface was rinsed in PBS pH 5.0 and water, and then dried with N2. Desorption was performed by immersing the samples in PBS with a high pH (high enough to fully desorb the protein in question based on SPR measurements). Alternatively, electrochemical release was carried out in a beaker, with a Pt cage as counter electrode and

Ag/AgCl as reference electrode. The reference electrode was prepared by depositing chloride ions onto a bare silver wire electrochemically by applying a +0.5 V for 10 min in 1 M HCl.

Fluorescence microscopy:

All fluorescence measurements were conducted using a Zeiss Axio Observer 7 inverted microscope equipped with an Axiocam506 camera. Microelectrodes in air were imaged using a 10× objective. The background fluorescence was measured on the unfunctionalized glass surface region next to the electrodes for each dye excitation/emission filter set and subtracted from the values obtained from the electrodes.

Protein conjugation:

Two different fluorophores were used in the conjugation of fluorescent dyes to the amines of BSA: Alexa Fluor 488 and 555 (with tetrafluorophenyl or N-hydroxysuccinimide ester groups). A BSA solution (100 µL, 10 mg/mL, pH 8.5) was mixed with Alexa Fluor dye (100 µg), and the resulting solution was inverted every 10 min for 1 h. The reaction was terminated by the addition of PBS pH 5.0, which reduced the pH to 5.0 and diluted the sample to a protein concentration of 0.2 mg/mL. The fluorescent proteins were immobilized in PMAA brushes in the same manner as the native proteins.

Vesicle preparation:

Vesicles were prepared using established methods.[38] In brief, the lipids were dried onto the interior of a glass vial by letting the solvent evaporate, followed by rehydration in buffer and extrusion through polycarbonate track-etched membranes with a diameter of 100 nm.

Acknowledgments

We thank Prof. Fredrik Höök and Mattias Sjöberg at the Dept. of Physics for supplying liposomes and discussing the results. Scott Mazurkewich at the Dept. of Biology is acknowledged for use of equipment.

Funding:

Financial support from the Knut & Alice Wallenberg Foundation (Academy Fellow 2015.0161), the Swedish Research Council (project grant 2016-03319) and the Erling-Persson Family Foundation is gratefully acknowledged.

Author contributions:

The concept was perceived by GFD and AD. GFD performed the majority of the experiments. ZAK introduced the aryl diazonium linker. RH performed NMR analysis. TR performed BSA-PEG conjugation. KX fabricated microelectrodes. AD was project leader. The manuscript was written with input from all authors.

Competing interests:

GFD and AD have applied for a patent of the technology.

Supplementary Materials

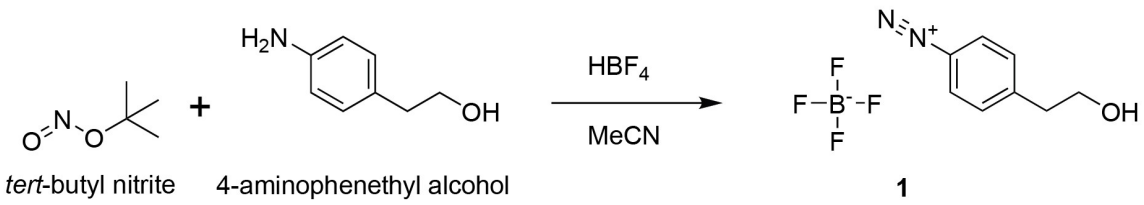

tert-butyl nitrite 4-aminophenethyl alcohol **1**

Fig. S1. Synthesis of diazonium salt **1.**

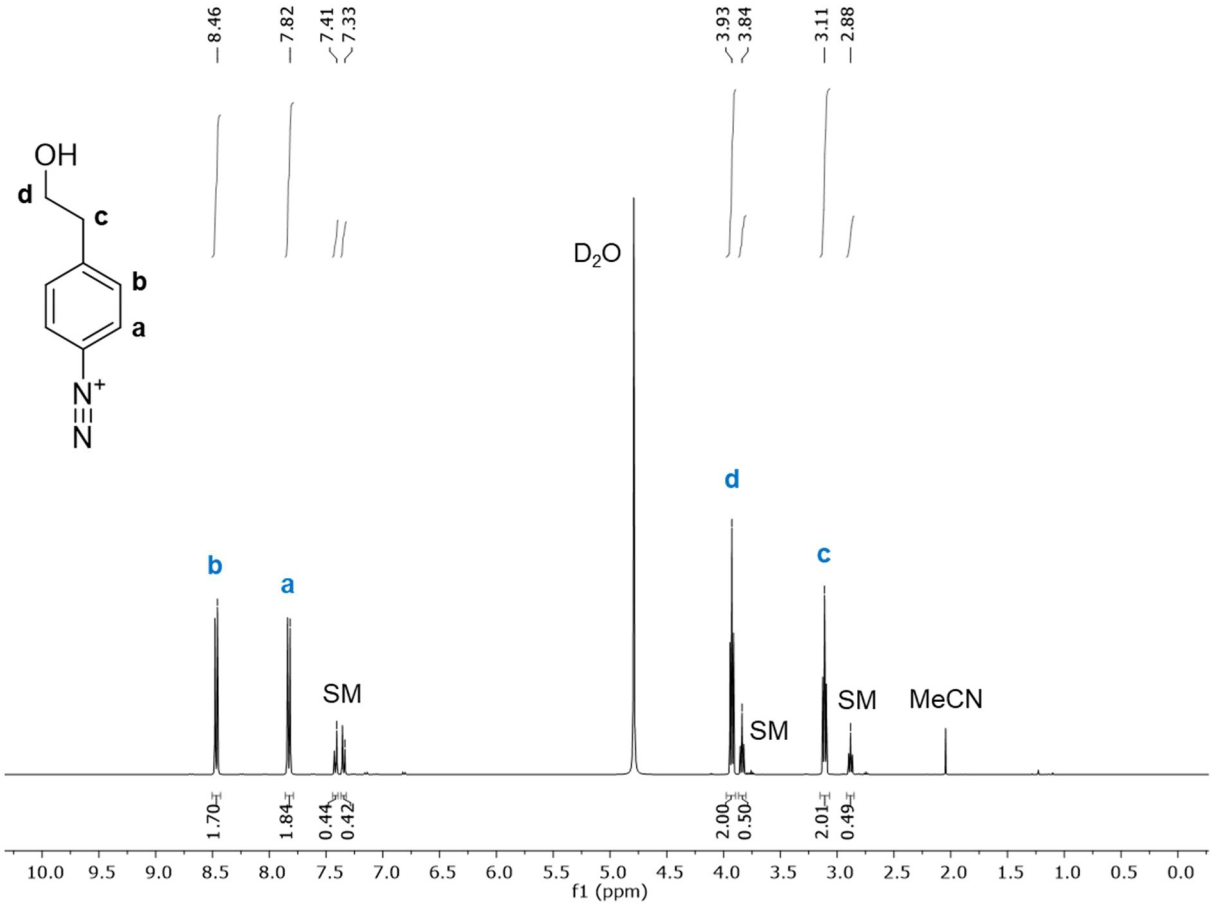

^{1}H NMR (400 MHz, D_2O) spectrum of diazonium salt **1**, where SM represents the starting material 4-aminophenethyl alcohol.

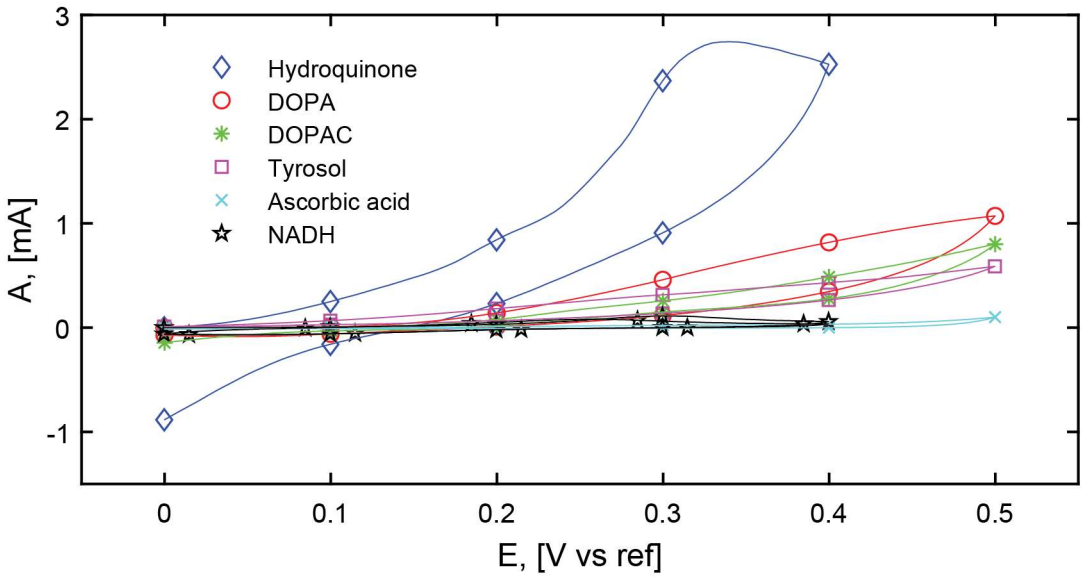

Fig. S2. CV (100 mV/s) where the oxidation peak is shown for different reducing agents. The electrode area was 0.78 cm^2 and the concentration of the species was 5 mM (in PBS pH 7.4) in each case. Faradaic currents are observed in most cases. For DOPA, the redox activity was quite strong but an organic coating was formed during potential application which quickly made Faradaic reactions impossible. The other species are capable of acidification but hydroquinone is clearly the most efficient.

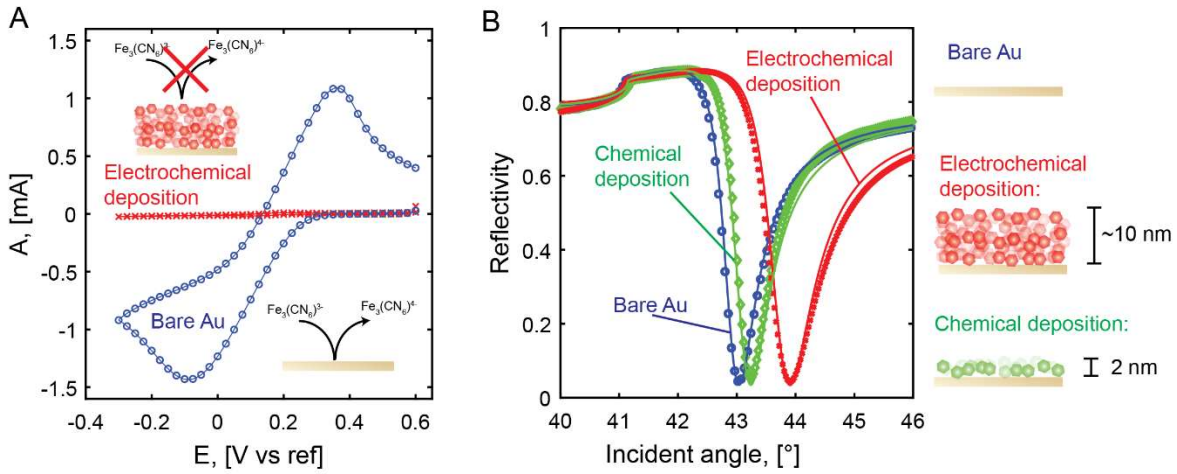

Fig. S3. Electrochemical attachment of diazonium salts does not produce an interface capable of Faradaic reactions. **(A)** CV scans (100 mV/s) in the presence of 5 mM ferrocyanide before and after electrografting, showing no current after layer formation. **(B)** SPR scans in air comparing chemical attachment (used in this work) with electrografting (one potential sweep between 0 V to −1 V). The electrografted layer is much thicker and blocks electron transfer.

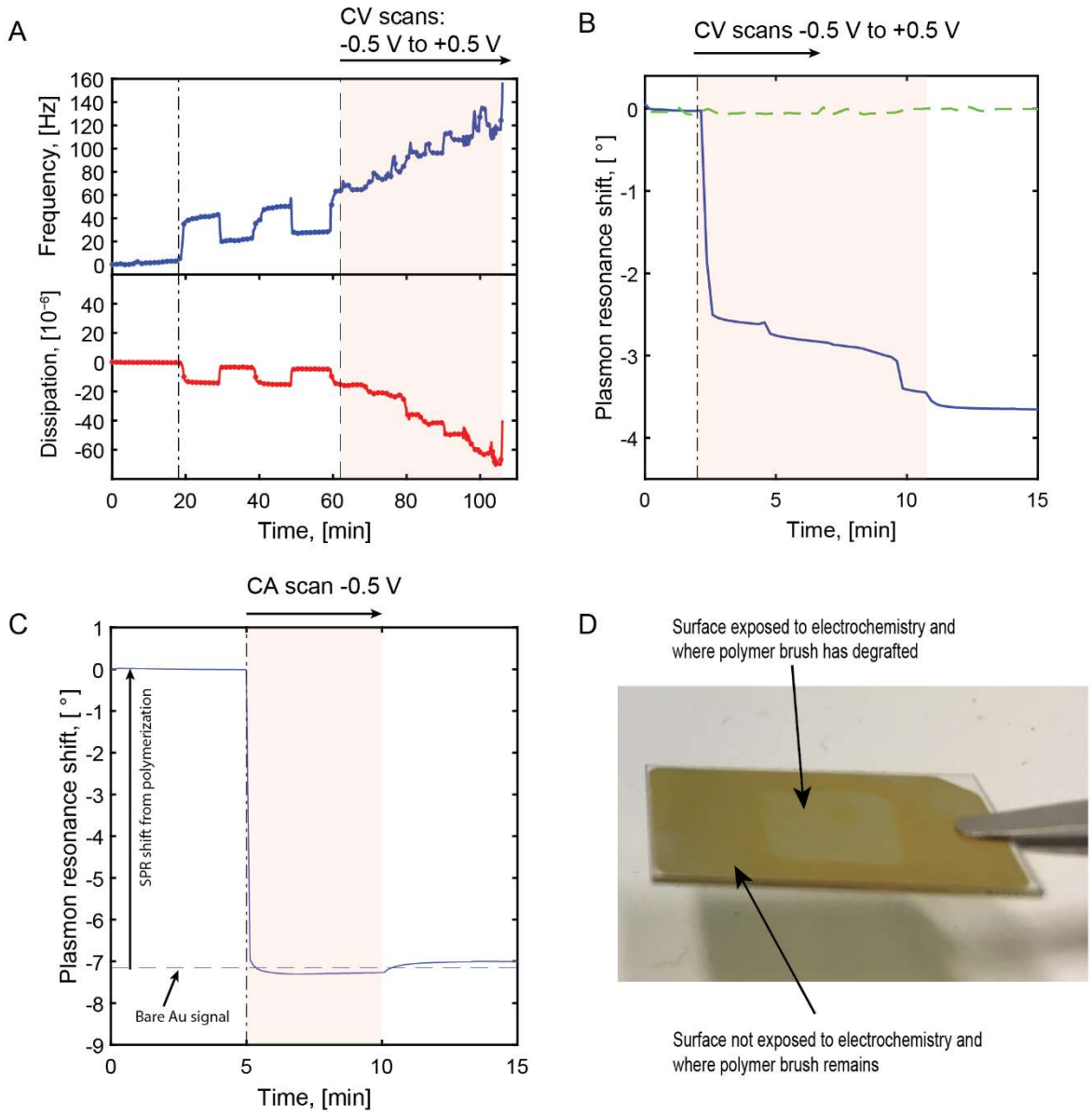

Fig. S4. Demonstration of instability of thiol linkers to gold electrodes upon applying electrochemical potentials. **(A)** QCM measurement where initially a polyelectrolyte brush is switched twice by changing the pH by pumping different buffers, followed by a time period (shaded region) where attempts are made to non-destructively perform CV sweeps within the potential range −0.5 to +0.5 V vs Ag/AgCl to achieve local pH gradients on the electrode surface. Material clearly leaves the surface. **(B)** Electrochemical SPR measurement where the same trend is observed. The time at which the electrochemical signal is applied is indicated and the corresponding SPR signal of a bare Au sensor is shown. **(C)** Electrochemical SPR experiment where a constant potential of −0.5 V is applied for 5 min. Total desorption of the brush is observed within seconds as verified by a control Au surface. **(D)** Photo of the SPR sensor surface from **(C)**. The thiol-anchored polyelectrolyte brush is visibly degrafted from the region of the surface exposed to liquid.

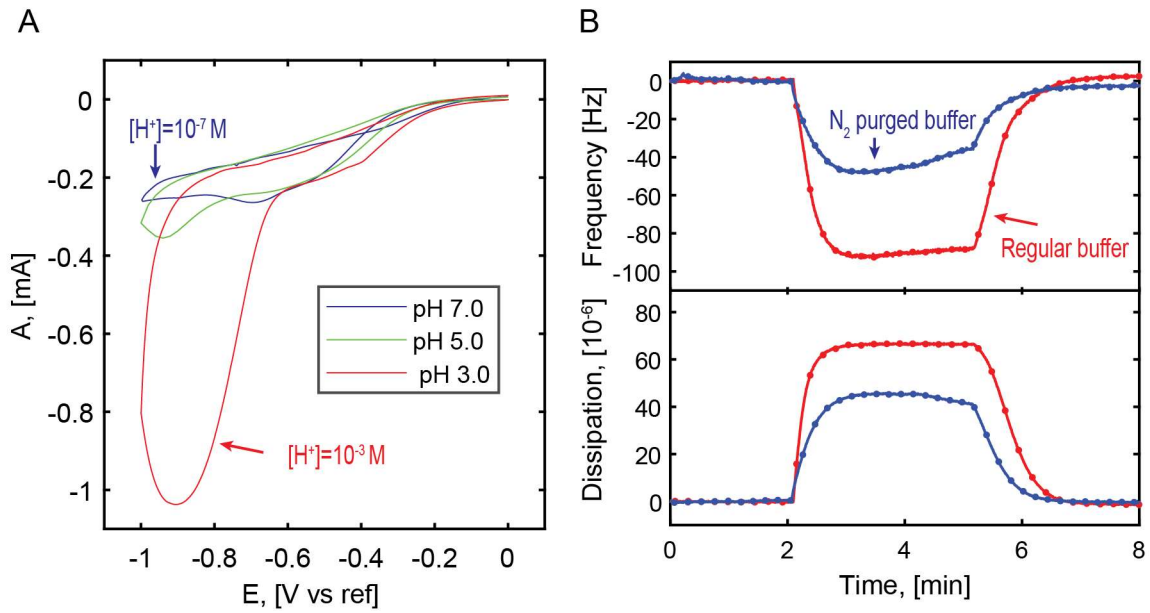

Fig. S5. (A) In-situ QCM CV scans (100 mV/s) of PMAA brushes measured at different pH. The electrode area was 0.78 cm^2. A higher current for the negative sweep is obtained at lower pH, showing that protons contribute to the Faradaic reaction. **(B)** QCM signals for a PMAA brush when an electrochemical potential is applied in a buffer with normal O_2 content (in equilibrium with ambient air) compared to an O_2 depleted buffer (buffer purged with N_2). The brush cannot be fully switched after N_2 purge.

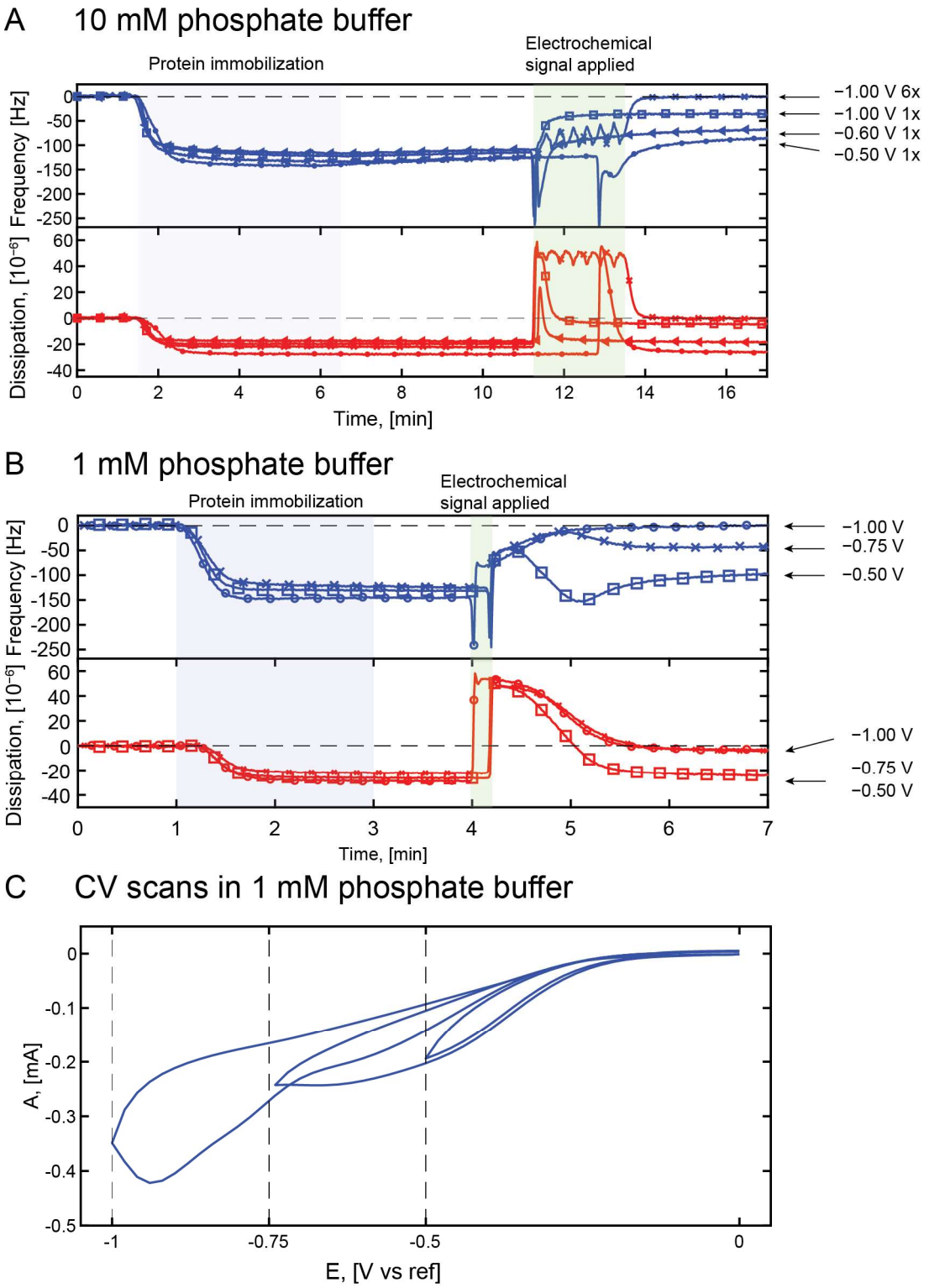

Fig. S6. BSA immobilization to PMAA followed by electrochemical desorption by CV scans in PBS pH 5. **(A)** 10 mM (standard) buffer strength. **(B)** 1 mM buffer strength. Dashed horizontal lines represent the baseline. **(C)** Corresponding CV scans obtained from the experiment in **(B)**. The results show that for the higher buffering capacity in **(A)**, a higher magnitude of potential sweep and increased number of cycles is required for full protein release.

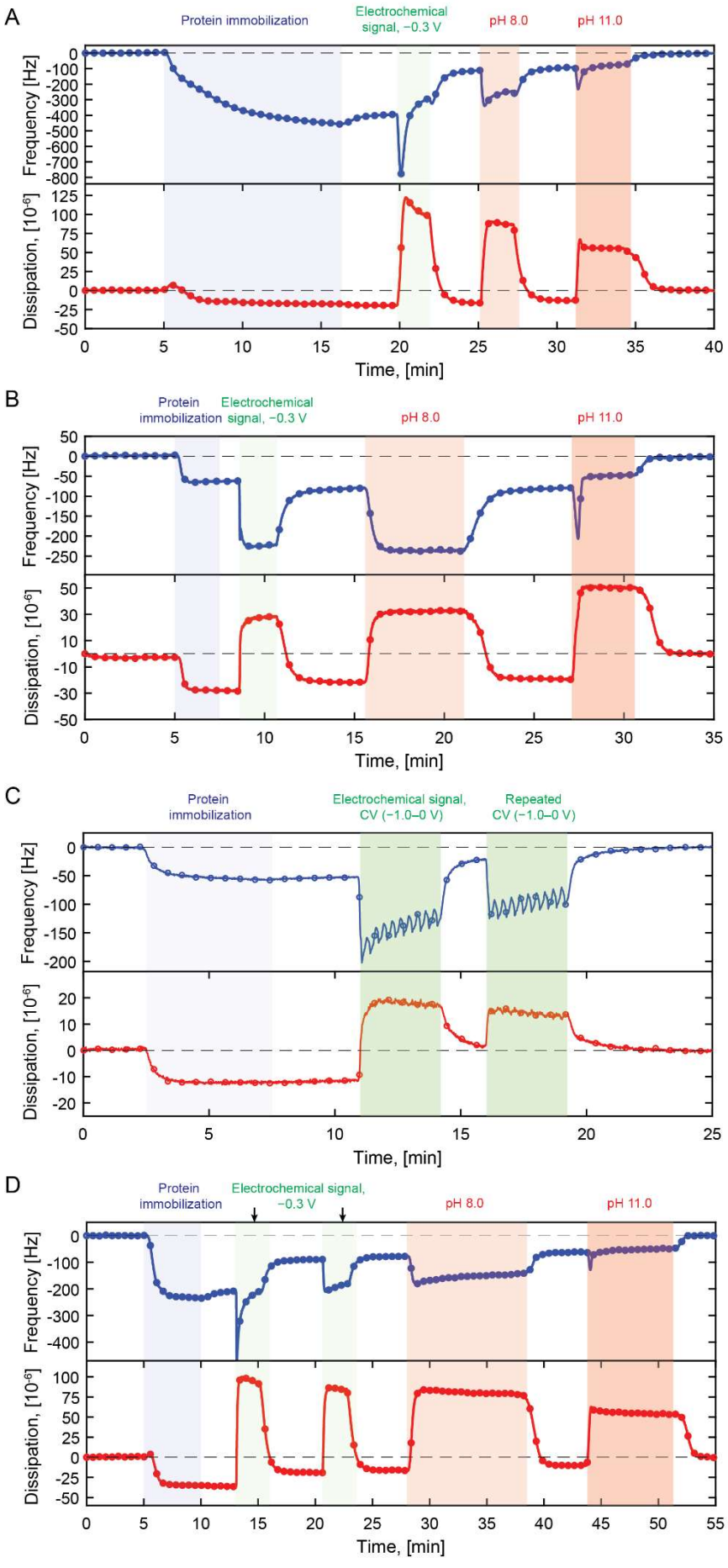
A
Protein immobilization
Electrochemical signal, −0.3 V
pH 8.0
pH 11.0
Frequency [Hz]
Dissipation, [10-6]
Time, [min]
B
Protein immobilization
Electrochemical signal, −0.3 V
pH 8.0
pH 11.0
Frequency [Hz]
Dissipation, [10-6]
Time, [min]
C
Protein immobilization
Electrochemical signal, CV (−1.0–0 V)
Repeated CV (−1.0–0 V)
Frequency [Hz]
Dissipation, [10-6]
Time, [min]
D
Protein immobilization
Electrochemical signal, −0.3 V
pH 8.0
pH 11.0
Frequency [Hz]
Dissipation, [10-6]
Time, [min]

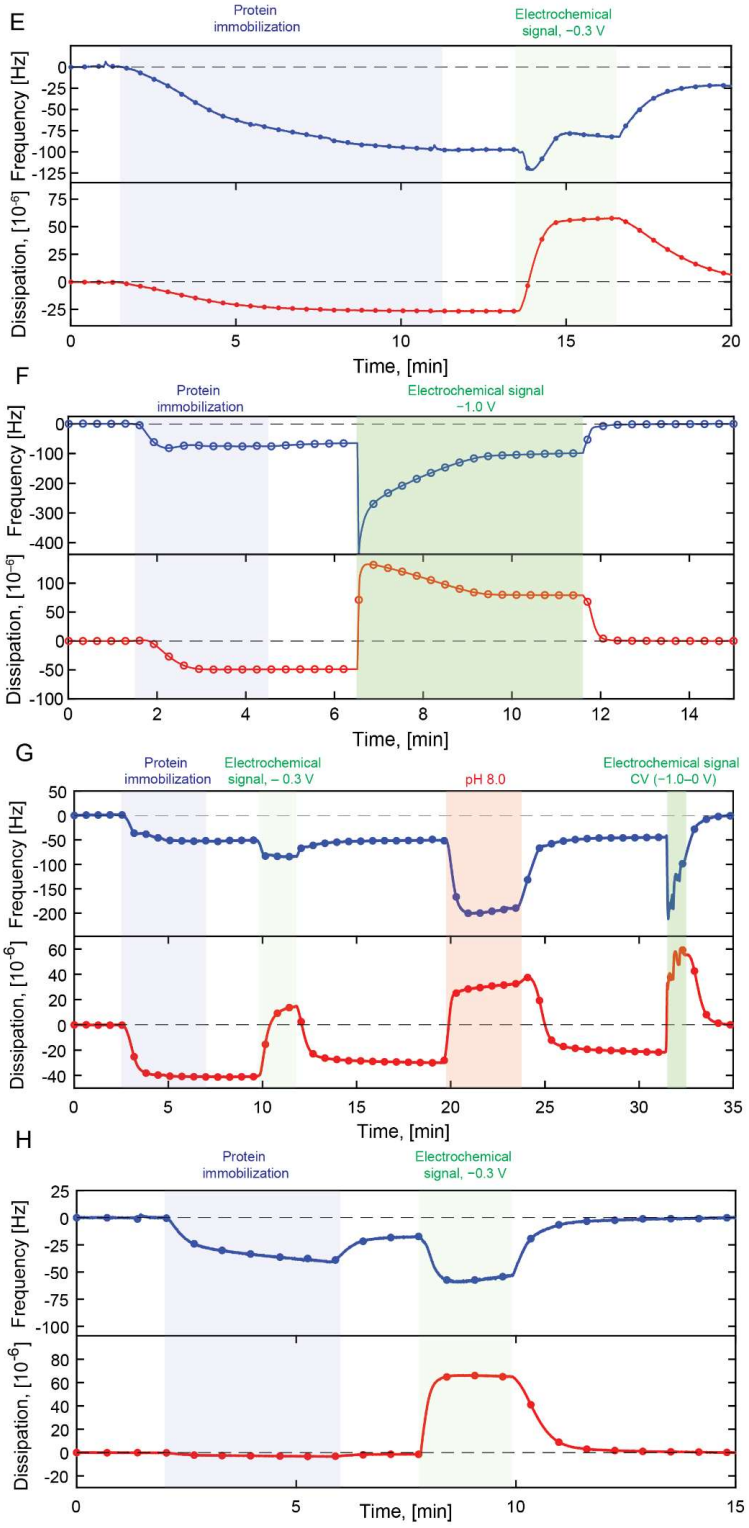

Fig. S7. Examples of proteins immobilized to PMAA and desorbed by increasing the local pH at the electrode interface by application of electrochemical potentials. The response from changing buffer pH is also shown in some cases. **(A)** FIB, **(B)** AVI chronoamperometry, **(C)** AVI desorption by CV, **(D)** NAVI, **(E)** INS, **(F)** INS glargine, **(G)** LYS and **(H)** HRP. Note that raising the pH of the buffers does not leads to desorption for proteins with high pI due to electrostatic interactions. The response seen is instead due to the deprotonation of the brush.

References

1. Stuart, M. A.; Huck, W. T.; Genzer, J.; Muller, M.; Ober, C.; Stamm, M.; Sukhorukov, G. B.; Szleifer, I.; Tsukruk, V. V.; Urban, M.; Winnik, F.; Zauscher, S.; Luzinov, I.; Minko, S., Emerging applications of stimuli-responsive polymer materials. *Nat Mater* **2010,** *9* (2), 101-13.
2. Jain, P.; Baker, G. L.; Bruening, M. L., Applications of polymer brushes in protein analysis and purification. *Annu Rev Anal Chem* **2009,** *2*, 387-408.
3. Tibbitt, M. W.; Dahlman, J. E.; Langer, R., Emerging Frontiers in Drug Delivery. *J Am Chem Soc* **2016,** *138* (3), 704-17.
4. Shukla, A. A.; Hubbard, B.; Tressel, T.; Guhan, S.; Low, D., Downstream processing of monoclonal antibodies--application of platform approaches. *J Chromatogr B Analyt Technol Biomed Life Sci* **2007,** *848* (1), 28-39.
5. Low, D.; O'Leary, R.; Pujar, N. S., Future of antibody purification. *J Chromatogr B Analyt Technol Biomed Life Sci* **2007,** *848* (1), 48-63.
6. Jonkheijm, P.; Weinrich, D.; Schroder, H.; Niemeyer, C. M.; Waldmann, H., Chemical strategies for generating protein biochips. *Angew Chem Int Ed Engl* **2008,** *47* (50), 9618-47.
7. Krishnamoorthy, M.; Hakobyan, S.; Ramstedt, M.; Gautrot, J. E., Surface-initiated polymer brushes in the biomedical field: applications in membrane science, biosensing, cell culture, regenerative medicine and antibacterial coatings. *Chem Rev* **2014,** *114* (21), 10976-1026.
8. Kuchler, A.; Yoshimoto, M.; Luginbuhl, S.; Mavelli, F.; Walde, P., Enzymatic reactions in confined environments. *Nat Nanotechnol* **2016,** *11* (5), 409-20.
9. Ellis, G. A.; Klein, W. P.; Lasarte-Aragonés, G.; Thakur, M.; Walper, S. A.; Medintz, I. L., Artificial Multienzyme Scaffolds: Pursuing in Vitro Substrate Channeling with an Overview of Current Progress. *ACS Catalysis* **2019,** *9* (12), 10812-10869.
10. Huber, D. L.; Manginell, R. P.; Samara, M. A.; Kim, B. I.; Bunker, B. C., Programmed adsorption and release of proteins in a microfluidic device. *Science* **2003,** *301* (5631), 352-4.
11. Katz, E.; Pingarron, J. M.; Mailloux, S.; Guz, N.; Gamella, M.; Melman, G.; Melman, A., Substance Release Triggered by Biomolecular Signals in Bioelectronic Systems. *J Phys Chem Lett* **2015,** *6* (8), 1340-7.
12. Anselmo, A. C.; Gokarn, Y.; Mitragotri, S., Non-invasive delivery strategies for biologics. *Nat Rev Drug Discov* **2019,** *18* (1), 19-40.
13. Mitragotri, S.; Burke, P. A.; Langer, R., Overcoming the challenges in administering biopharmaceuticals: formulation and delivery strategies. *Nat Rev Drug Discov* **2014,** *13* (9), 655-72.
14. Tam, T. K.; Pita, M.; Trotsenko, O.; Motornov, M.; Tokarev, I.; Halamek, J.; Minko, S.; Katz, E., Reversible "closing" of an electrode interface functionalized with a polymer brush by an electrochemical signal. *Langmuir* **2010,** *26* (6), 4506-13.
15. Bellare, M.; Kadambar, V. K.; Bollella, P.; Gamella, M.; Katz, E.; Melman, A., Electrochemical Signal-triggered Release of Biomolecules Functionalized with His-tag Units. *Electroanalysis* **2019,** *31* (11), 2274-2282.
16. Staples, M.; Daniel, K.; Cima, M. J.; Langer, R., Application of micro- and nano-electromechanical devices to drug delivery. *Pharm Res* **2006,** *23* (5), 847-63.
17. Santini, J. T., Jr.; Cima, M. J.; Langer, R., A controlled-release microchip. *Nature* **1999,** *397* (6717), 335-8.
18. Farra, R.; Sheppard, N. F., Jr.; McCabe, L.; Neer, R. M.; Anderson, J. M.; Santini, J. T., Jr.; Cima, M. J.; Langer, R., First-in-human testing of a wirelessly controlled drug delivery microchip. *Sci Transl Med* **2012,** *4* (122), 122ra21.
19. Bellare, M.; Kadambar, V. K.; Bollella, P.; Katz, E.; Melman, A., Electrochemically stimulated molecule release associated with interfacial pH changes. *Chem Commun (Camb)* **2019,** *55* (54), 7856-7859.

20. Ghaly, T.; Wildt, B. E.; Searson, P. C., Electrochemical release of fluorescently labeled thiols from patterned gold surfaces. *Langmuir* **2010,** *26* (3), 1420-3.
21. Hodneland, C. D.; Mrksich, M., Biomolecular Surfaces that Release Ligands under Electrochemical Control. *Journal of the American Chemical Society* **2000,** *122* (17), 4235-4236.
22. Wang, F.; Li, D.; Li, G.; Liu, X.; Dong, S., Electrodissolution of inorganic ions/DNA multilayer film for tunable DNA release. *Biomacromolecules* **2008,** *9* (10), 2645-52.
23. Gamella, M.; Zakharchenko, A.; Guz, N.; Masi, M.; Minko, S.; Kolpashchikov, D. M.; Iken, H.; Poghossian, A.; Schöning, M. J.; Katz, E., DNA Computing Systems Activated by Electrochemically-triggered DNA Release from a Polymer-brush-modified Electrode Array. *Electroanalysis* **2016**.
24. Honarvarfard, E.; Gamella, M.; Channaveerappa, D.; Darie, C. C.; Poghossian, A.; Schöning, M. J.; Katz, E., Electrochemically Stimulated Insulin Release from a Modified Graphene-functionalized Carbon Fiber Electrode. *Electroanalysis* **2017,** *29* (6), 1543-1553.
25. Zhu, H.; Yan, J.; Revzin, A., Catch and release cell sorting: electrochemical desorption of T-cells from antibody-modified microelectrodes. *Colloids Surf B Biointerfaces* **2008,** *64* (2), 260-8.
26. Talbert, J. N.; Goddard, J. M., Enzymes on material surfaces. *Colloids Surf B Biointerfaces* **2012,** *93*, 8-19.
27. Takasu, K.; Kushiro, K.; Hayashi, K.; Iwasaki, Y.; Inoue, S.; Tamechika, E.; Takai, M., Polymer brush biointerfaces for highly sensitive biosensors that preserve the structure and function of immobilized proteins. *Sensors and Actuators B: Chemical* **2015,** *216*, 428-433.
28. Shastri, A.; McGregor, L. M.; Liu, Y.; Harris, V.; Nan, H.; Mujica, M.; Vasquez, Y.; Bhattacharya, A.; Ma, Y.; Aizenberg, M.; Kuksenok, O.; Balazs, A. C.; Aizenberg, J.; He, X., An aptamer-functionalized chemomechanically modulated biomolecule catch-and-release system. *Nat Chem* **2015,** *7* (5), 447-54.
29. Di Palma, G.; Kotowska, A. M.; Hart, L. R.; Scurr, D. J.; Rawson, F. J.; Tommasone, S.; Mendes, P. M., Reversible, High-Affinity Surface Capturing of Proteins Directed by Supramolecular Assembly. *ACS Appl Mater Interfaces* **2019,** *11* (9), 8937-8944.
30. Schweizer, D.; Schonhammer, K.; Jahn, M.; Gopferich, A., Protein-polyanion interactions for the controlled release of monoclonal antibodies. *Biomacromolecules* **2013,** *14* (1), 75-83.
31. Kusumo, A.; Bombalski, L.; Lin, Q.; Matyjaszewski, K.; Schneider, J. W.; Tilton, R. D., High capacity, charge-selective protein uptake by polyelectrolyte brushes. *Langmuir* **2007,** *23* (8), 4448-54.
32. Sun, L.; Dai, J.; Baker, G. L.; Bruening, M. L., High-Capacity, Protein-Binding Membranes Based on Polymer Brushes Grown in Porous Substrates. *Chemistry of Materials* **2006,** *18* (17), 4033-4039.
33. Gam-Derouich, S.; Ngoc Nguyen, M.; Madani, A.; Maouche, N.; Lang, P.; Perruchot, C.; Chehimi, M. M., Aryl diazonium salt surface chemistry and ATRP for the preparation of molecularly imprinted polymer grafts on gold substrates. *Surface and Interface Analysis* **2010,** *42* (6-7), 1050-1056.
34. Ferrand-Drake del Castillo, G.; Emilsson, G.; Dahlin, A., Quantitative Analysis of Thickness and pH Actuation of Weak Polyelectrolyte Brushes. *The Journal of Physical Chemistry C* **2018,** *122* (48), 27516-27527.
35. Fomina, N.; Johnson, C. A.; Maruniak, A.; Bahrampour, S.; Lang, C.; Davis, R. W.; Kavusi, S.; Ahmad, H., An electrochemical platform for localized pH control on demand. *Lab Chip* **2016,** *16* (12), 2236-44.
36. Pinson, J.; Podvorica, F., Attachment of organic layers to conductive or semiconductive surfaces by reduction of diazonium salts. *Chem Soc Rev* **2005,** *34* (5), 429-39.
37. Castillo, G. F.-D. d.; Adali-Kaya, Z.; Hailes, R. L. N.; Robson, T.; Dahlin, A., Generic High-Capacity Protein Capture and Release by pH Control. *Submitted and under revision* **2020**.

38. Graneli, A.; Edvardsson, M.; Hook, F., DNA-based formation of a supported, three-dimensional lipid vesicle matrix probed by QCM-D and SPR. *Chemphyschem* **2004,** *5* (5), 729-33.
39. Sabate Del Rio, J.; Henry, O. Y. F.; Jolly, P.; Ingber, D. E., An antifouling coating that enables affinity-based electrochemical biosensing in complex biological fluids. *Nat Nanotechnol* **2019,** *14* (12), 1143-1149.
40. Salatino, J. W.; Ludwig, K. A.; Kozai, T. D. Y.; Purcell, E. K., Glial responses to implanted electrodes in the brain. *Nat Biomed Eng* **2017,** *1* (11), 862-877.
41. Gutowski, S. M.; Shoemaker, J. T.; Templeman, K. L.; Wei, Y.; Latour, R. A., Jr.; Bellamkonda, R. V.; LaPlaca, M. C.; Garcia, A. J., Protease-degradable PEG-maleimide coating with on-demand release of IL-1Ra to improve tissue response to neural electrodes. *Biomaterials* **2015,** *44*, 55-70.
42. Okutucu, B.; Dincer, A.; Habib, O.; Zihnioglu, F., Comparison of five methods for determination of total plasma protein concentration. *J Biochem Biophys Methods* **2007,** *70* (5), 709-11.
43. Xiong, K.; Emilsson, G.; Dahlin, A. B., Biosensing using plasmonic nanohole arrays with small, homogenous and tunable aperture diameters. *Analyst* **2016,** *141* (12), 3803-10.
44. Dong, R.; Krishnan, S.; Baird, B. A.; Lindau, M.; Ober, C. K., Patterned biofunctional poly(acrylic acid) brushes on silicon surfaces. *Biomacromolecules* **2007,** *8* (10), 3082-92.
45. Young, J. F.; Nguyen, H. D.; Yang, L.; Huskens, J.; Jonkheijm, P.; Brunsveld, L., Strong and reversible monovalent supramolecular protein immobilization. *Chembiochem* **2010,** *11* (2), 180-3.
46. Wasserberg, D.; Cabanas-Danes, J.; Subramaniam, V.; Huskens, J.; Jonkheijm, P., Orthogonal supramolecular protein assembly on patterned bifunctional surfaces. *Chem Commun (Camb)* **2018,** *54* (13), 1615-1618.
47. Wasserberg, D.; Nicosia, C.; Tromp, E. E.; Subramaniam, V.; Huskens, J.; Jonkheijm, P., Oriented protein immobilization using covalent and noncovalent chemistry on a thiol-reactive self-reporting surface. *J Am Chem Soc* **2013,** *135* (8), 3104-11.
48. Ferrand-Drake Del Castillo, G.; Koenig, M.; Muller, M.; Eichhorn, K. J.; Stamm, M.; Uhlmann, P.; Dahlin, A., Enzyme Immobilization in Polyelectrolyte Brushes: High Loading and Enhanced Activity Compared to Monolayers. *Langmuir* **2019,** *35* (9), 3479-3489.